

Analysis and Research on Working Performance of Shearer Based on Discrete Element Method

ZHIZHONG XING^{ID} AND WEI GUO

College of Mechanical Engineering, Xi'an University of Science and Technology, Xi'an 710054, China

Corresponding author: Wei Guo (guow@xust.edu.cn)

This work was supported in part by the National Key Research and Development Program of China under Grant 2017YFC0804310.

ABSTRACT In view of the complex nonlinear relationship between the shearer mining rate and the cutting specific energy consumption in a fully mechanized mining face, the optimal combination of shearer motion parameters and geometric parameters is studied to achieve green mining by improving the coal mining rate and reducing the cutting specific energy consumption. The orthogonal virtual test of the shearer's working performance is carried out using the discrete element software EDEM. The evaluation indexes of the shearer's working performance are the coal mining rate and the cutting specific energy consumption. The results of the research based on the discrete element method are analyzed by the regression method. The regression equation of the evaluation indexes is calculated by SPSS software, and the three-dimensional contour map is drawn by MATLAB. The influence rule of the research factors on the evaluation index is determined. By optimizing the evaluation index, the optimal combination of parameters after shearer rounding is obtained: the drum speed is 74.1 r/min, the hub diameter is 321.8 mm, and the pick angle is 22.3°. The coal mining rate is 80.71%, and the cutting specific energy consumption is 585.64 w · h/m³. The simulation results are verified by experiments, which demonstrate the accuracy and feasibility of using the discrete element method to study the energy consumption of the shearer's mining rate and cutting ratio.

INDEX TERMS Shearer, discrete element, cutting specific energy consumption, mining rate, rotary orthogonal test.

I. INTRODUCTION

The shearer is one of the key pieces of equipment in the integrated manufacturing system of "three machines" in fully mechanized mining. Its working conditions are both bad and complex. There is a complex nonlinear relationship between the coal mining rate and the cutting specific energy consumption [1]–[3]. Searching for appropriate means and methods to carry out research on the shearer, by changing its motion parameters and geometric parameters to improve its coal mining performance and reduce its energy consumption, could not only conserve significant manpower and financial resources but also have far-reaching effects on the sustainable development of green coal mining [4]–[7].

The "three machines" of a fully mechanized mining face cooperate with each other; the shearer undertakes the task of coal breaking, and the scraper conveyor and hydraulic support undertake the tasks of coal transportation and support,

The associate editor coordinating the review of this article and approving it for publication was Chi-Tsun Cheng.

respectively. Fig. 1 is a schematic diagram of longwall mining by shearer in a fully mechanized mining face.

In Fig. 1, the shearer is close to the coal seam, and its body is mounted on the chute of the scraper conveyor. Driven by the haulage device, the shearer moves back and forth along the chute of the scraper conveyor to perform the coal cutting operation. The scraper conveyor is positioned along the coal seam and connected with the hydraulic support through the push jack, and the hydraulic support is responsible for conveying the scraper. At the same time, the hydraulic support timely follows up the roof of the shearer after the goaf.

As a key index for evaluating the working performance of the shearer, the coal mining rate directly affects the productivity, load fluctuation, tool wear, dust output and dynamic reliability of the shearer [8]–[14]. With the rapid development of the world economy and coal industry, more and more scholars and manufacturers have applied different methods to the study of fully mechanized mining face shearers. Most of the studies on shearer mining rate are theoretical research, tests and finite element analysis [8], [15]–[17]. Miller et al.

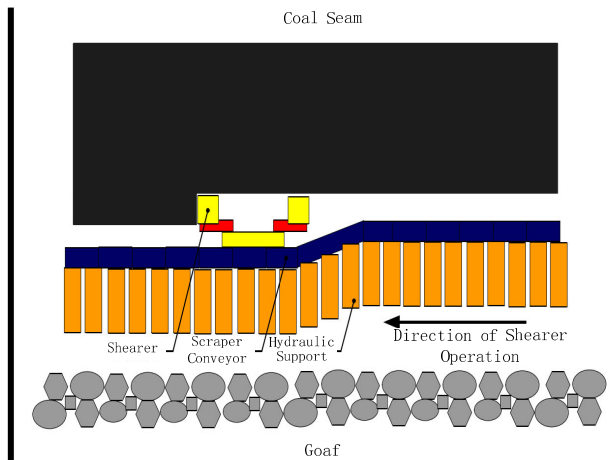


FIGURE 1. Diagram of longwall mining in a fully mechanized mining face.

studied the influence of hydraulic fracturing on the coal mining rate and constructed a method to improve the coal mining rate of thick and hard coal seams through pulse water prefracturing technology [18]. Li et al. studied the influence of drum steering on coal mining performance through theoretical and experimental research. The test results show that drum reversal is 2.03% [19] higher than that of forward steering. Freebairn et al. analyzed the mining mechanism of the shearer by the finite element method and, from the structural and kinematic parameters of the drum, analyzed the various factors affecting the mining rate of the shearer, obtaining the influence rules of the blade helical angle, traction speed and drum speed on mining performance by using a coal rock cutting test bench [20]. Sdvyzhkova et al. put forward an exponential curve shearer drum and carried out an experimental study on the drum. The results show that the shearer drum with this structure is 6% [21] higher than the cylindrical shearer drum. Svobodova et al. compared the mining effect of a conical cylinder hub drum and cylindrical cylinder hub drum via an underground test. The results show that the mining rate of the conical cylinder hub drum is higher than that of the cylindrical cylinder hub drum, and the lump coal rate of the conical cylinder hub drum is also significantly higher than that of the cylindrical cylinder hub drum [22]. Arteag et al. studied the influence of blade rotation and mining technology on the effect of small-diameter shearer drum mining by means of experiments and put forward the mining scheme of one-way coal cutting and one-knife round trip [23]. Tyulenev et al. designed four types of cutter arrangement drums for a cutting test. Through the test, the relationship between the cutter arrangement and the shearer mining rate was found [24]. However, a test of coal cutting and crushing process on the physical prototype has great data perturbation, which makes it difficult to accurately identify the required operating parameters and data acquisition. The traditional design and test cycle is long, the cost is high, and many hypotheses involved in the theoretical deduction are not consistent with the actual situation. Based on the traditional continuum mechanics, the finite element method

regards coal mining as continuous contact force, which is directly used to calculate and simulate the specific cutting and breaking process of coal and rock, and it cannot meet the analysis requirements. The coal and rock cut by a shearer drum is granular and has the property of granular matter. The discrete element method is the main method for solving the problem of the discontinuous granular group at present. From the previous studies and search results, it is known that, although the shearer's mining rate has been analyzed and discussed, it is still unknown how to improve the mining rate when considering the specific energy consumption of cutting. Therefore, this paper uses the discrete element method to study the combination of the shearer mining rate and the cutting specific energy consumption. The main contributions of this paper are summarized as follows:

(1) This paper takes the MG160/375-QWD shearer as the research carrier, regards high coal mining rate and low cutting specific energy consumption as the research objective, and develops the coal particle contact model in the discrete element method through an Application Programming Interface (API) (the EDEM API is used to customize and extend the functions of EDEM; the API uses standard C++ scripts to allow researchers to add features to new particle contact models, simulation characteristics, and custom particle factories, thus realizing various functions, such as particle breakage in simulation). The discrete element software EDEM is used to simulate the scheme of quadratic orthogonal rotation combination.

(2) The regression equation of the coal mining rate and cutting specific energy consumption is calculated by SPSS software, and the three-dimensional contour map is drawn by MATLAB. The influence law of the factors studied on the coal mining rate and cutting specific energy consumption is determined, and the optimal combination of parameters of the shearer with high efficiency and low consumption is obtained.

(3) The simulation results are verified by experiments, which show that it is feasible to use the discrete element method to analyze and optimize the energy consumption of the shearer's mining rate and cutting ratio. The research results provide theoretical reference and basis for rational design and selection of the shearer's motion parameters and geometric parameters in the future and promote the realization of green coal mining.

The rest of this paper is organized as follows. Section 2 introduces the particle contact model and kinematics model. Section 3 studies the working performance of the shearer based on EDEM. Section 4 presents the experimental verification, and section 5 summarizes the paper.

II. ESTABLISHMENT OF THE MODEL

A. DISCRETE ELEMENT MODEL

In the study of the discrete element method, the main contact models are the Hertz-Mindlin (no slip) built-in model, Hertz-Mindlin bond model, linear bond contact model, moving surface contact model, linear elastic contact model and frictional

charge contact model [25]. In this study, it is considered that there is no adhesion between particles, so the contact model between coal particles and shearer is the Hertz-Mindlin (no slip) built-in model [26]. The normal force between coal particles in the model is as follows:

$$F_n = \frac{4}{3}E^*(R^*)^{1/2}\alpha^{3/2} \quad (1)$$

In formula 1, R^* is the equivalent coal particle radius, α is the contact radius, and E^* is the equivalent elastic modulus. Its expression is as follows:

$$\frac{1}{E^*} = \frac{1 - \nu_1^2}{E_1} + \frac{1 - \nu_2^2}{E_2} \quad (2)$$

In formula 2, the elastic modulus and Poisson's ratio of coal particle 1 are E_1 and ν_1 , and the elastic modulus and Poisson's ratio of coal particle 2 are E_2 and ν_2 . The tangential force between coal particles is:

$$F_t = -8G^*\sqrt{R^*\alpha}\delta \quad (3)$$

In formula 3, δ is the tangential overlap, and G^* is the equivalent shear modulus, which is expressed as follows:

$$G^* = \frac{2 - \nu_1^2}{G_1} + \frac{2 - \nu_2^2}{G_2} \quad (4)$$

In formula 4, G_1 is the shear modulus of coal particle 1, and G_2 is the shear modulus of coal particle 2. Therefore, the settings of the elastic modulus, Poisson's ratio and shear modulus of the particles in the model will have an important influence on the calculation results based on the discrete element method.

B. MINING PROCESS MODEL

The contact between coal particles and shearer is mainly divided into two important parts: the drum pick and drum blade. Ignoring the gravity of coal particles, the force of coal particles on the pick of the drum is analyzed (Fig. 2).

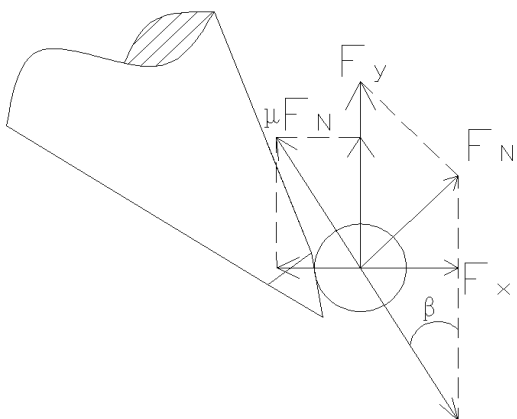


FIGURE 2. Force analysis of coal particles on the pick.

The force balance equation of coal particles is obtained as follows:

$$\begin{cases} F_x = F_N (\cos\beta - \mu \sin\beta) \\ F_y = F_N (\cos\beta + \mu \cos\beta) \end{cases} \quad (5)$$

In the formula, F_x is the axial coal throwing force, N ; F_y is the tangential force of coal particles, N ; μ is the friction coefficient; F_N is the supporting force of the pick on the coal particles, N ; β is the helical angle of the pick, ($^\circ$). The mining power of the drum can be obtained from formula 5 and the rotational speed:

$$P_z = \frac{[F_N (\sin\beta + \mu \cos\beta)] v_q}{1000} \quad (6)$$

In the formula, v_q is the tangential velocity of coal particles, m/s, and the drum mining power P_z in formula 6 can be expressed as:

$$P_z = \frac{0.1d_t v_m S_r}{n} \quad (7)$$

In the model, d_t is the rolling diameter of the shearer, mm; v_m is the cutting line speed of the shearer, m/s; S_r is the resistance coefficient; the values of the plates with and without stoppers are 420 and 1150, N/c m; n is the rotational speed of the shearer drum, r/min. Through the relationship between Formula 3 and Formula 4, it is concluded that:

$$F_N = \frac{100\cos\gamma_c d_t v_m S_r}{\pi n^2 d_l \sin\beta \sin(\beta + \gamma_c)(\sin\beta + \mu \cos\beta)} \quad (8)$$

In the formula, γ_c is the friction angle, ($^\circ$); d_l is the rotating diameter of coal particles, mm. By substituting formula 8 into formula 5, formulas 9 and 10 can be obtained as follows:

$$F_x = \frac{100((\cos\beta - \mu \sin\beta) \cos\gamma_c d_t v_m S_r)}{\pi n^2 d_l \sin\beta \sin(\beta + \gamma_c)(\sin\beta + \mu \cos\beta)} \quad (9)$$

$$F_y = \frac{100\cos\beta d_t v_m S_r}{\pi n^2 d_l \sin\beta \sin(\beta + \gamma_c)} \quad (10)$$

Thus far, it can be concluded that the force movement of coal particles on the pick is affected by the complex combination of multiple parameters, such as pick angle β , hub diameter d_t and drum speed n .

In addition, the movement process of coal particles on the blade is analyzed (and when there are too many coal particles, blockage may occur, which may affect the coal mining rate). The contact and separation motion between the cut coal and the drum blade is expressed by the Markov stochastic process method, and the falling process is expressed by the Kolmogorov differential-difference equation [27], that is,

$$\frac{dP_{N_b}(t)}{dt} = -\gamma_{N_b} P_{N_b}(t) + \gamma_{N_{b-1}} P_{N_{b-1}}(t) \quad (11)$$

In the formula, N_f is a random value representing the number of coal particles on the drum blade at time t_1 .

$P_{N_b}(t)$ is the probability of the random value N_f being set to the integer value N_b , that is, γ_{N_b} is a constant.

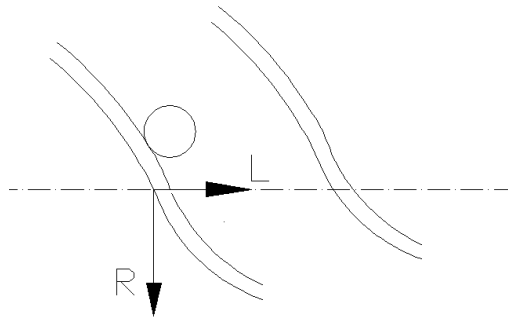


FIGURE 3. A sketch of the drum blade.

The diffusion behavior of coal particles on the drum blade (Fig. 3) is finally expressed by the Kolmogorov equation, which is as follows:

$$\frac{\partial M}{\partial t} = -v \frac{\partial M}{\partial L} + c_1 \frac{\partial^2 M}{\partial L^2} + \frac{c_2}{R} \frac{\partial}{\partial R} \left(R \frac{\partial M}{\partial R} \right) \quad (12)$$

The above formula describes the movement behavior of discrete coal particles on the drum blade during the random diffusion process. M is the total mass of coal between different blades, kg; t is the working time, s; V is the velocity of coal particles along the axis of the drum, m/s; c_1 is the movement coefficient of coal particles along the axis of the drum, c_2 is the radial movement coefficient of coal particles along the drum, L is the coordinate corresponding to the axial dimension of the shearer drum, R is the coordinate corresponding to the radial dimension of the shearer drum, and c_1 and c_2 are affected by the geometrical size of the particle and the rotational speed of the drum. However, considering the relatively harsh mining environment, the rotation of the drum destroys the continuity of particle behavior [5]. Therefore, the movement form of coal particles at cutting time and the movement form of coal particles on the drum blade are affected by many factors. This paper studies the main factors affecting the coal mining rate and cutting specific energy consumption: drum speed, drum hub diameter and pick elevation angle.

III. STUDY OF THE WORKING PERFORMANCE OF THE SHEARER BASED ON EDEM

A. ESTABLISHMENT OF THE GEOMETRIC MODEL AND COAL AND ROCK MATERIALS

In view of the weak modeling ability of the discrete element software EDEM itself, the simulation research based on the discrete element method only needs to import the external geometry that contacts the coal particle into [14], [28], [29]. To ensure the efficiency of the simulation calculation, the geometric dimensions of the MG160/375-QWD shearer drum were measured, and the simplified shearer drum was modeled by UG software (Fig. 4).

The coal wall cut by the shearer in the actual working process contains coal and rock. Therefore, to more accurately

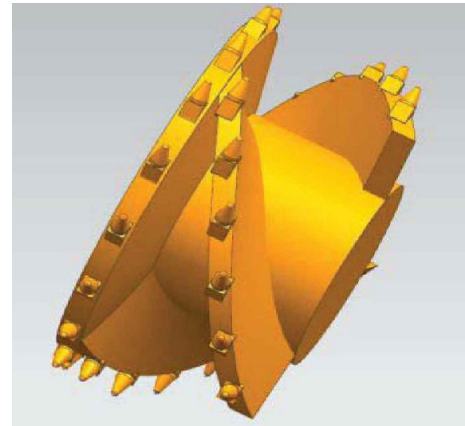


FIGURE 4. UG model of the shearer drum.



FIGURE 5. Coal and rock samples.

analyze the coal mining rate and cutting specific energy consumption, the artificial coal wall is made by mixing coal powder, rock and water at a ratio of 5:2:1 [30]. The resulting coal and rock samples are shown in Fig. 5.

B. PARTICLE MODEL TESTING AND DISCRETE ELEMENT METHOD SIMULATION

According to the collapse test, the angle of repose of coal and rock particles is tested, and the results of the angle of repose test are input to the online testing tool of the EDEM official website to obtain the relevant data of the physical and mechanical properties of coal and rock particles. Based on the literature, the physical and mechanical properties of coal and rock particles and pick, blade and roller are set up, as shown in Tables 1 and 2 [31]–[34].

TABLE 1. Physical characteristics.

Material	Density (kg/m ³)	Poisson ratio	Shear modulus (Pa)
Coal and rock particles	1315	0.24	1.83×10^8
Pick tooth	8200	0.39	3.12×10^9
Blade and drum	7800	0.33	3.11×10^{11}

TABLE 2. Mechanical properties.

Interaction	Static friction coefficient	Dynamic friction coefficient	Collision Recovery Coefficient
Coal and rock particles and picks	0.35	0.02	0.41
Coal and rock particles and blades and rollers	0.37	0.04	0.43
Coal-rock particles and coal-rock particles	0.44	0.09	0.52

Although the Hertz-MindLin (no slip) built-in model is known as the contact model between coal and rock particles and the pick, in view of the small bonding effect between coal and rock particles, the JKR contact model in EDEM can better complete the bonding of particles. To ensure that the selected contact model is more suitable for the particles studied and achieve the effect of coal crushing and mining, the JKR contact model is developed by secondary programming using the application programming interface (API). Under the impact of the pick on the coal body based on the discrete element method, the X, Y and Z directions of tensile fracture and shear fracture between particles are as shown in Fig. 6 and Fig. 7.

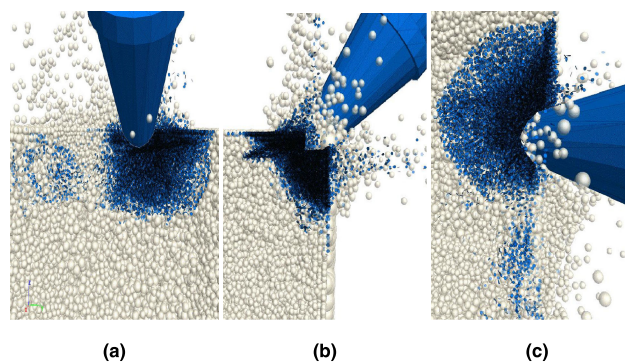


FIGURE 6. Tensile fracture between coal and rock particles. (a) X-directional view of tensile fracture. (b) Y-directional view of tensile fracture. (c) Z-directional view of tensile fracture.

From Fig. 6 and Fig. 7, it can be seen that the contact model developed by the API can better realize the mining process of coal and rock particles being broken by using different colors to mark the tensile fracture and shear fracture of coal and rock particles in the X, Y and Z directions. To better verify the feasibility of particle breakage simulation by the discrete element method and the compiled JKR model, the coal breakage by the pick is analyzed from a macroscopic point of view. In the discrete element software, the cutter is ordered to collide with the coal and rock mass with a certain motion, as shown in Fig. 8 (a). When the cutting force of the pick exceeds the bonding force between particles (the bonding force is obtained by simulation and experimental calibration, and the result is 1.9×10^6 N) [35], the coal and rock mass is broken as shown in Fig. 8 (b), in which

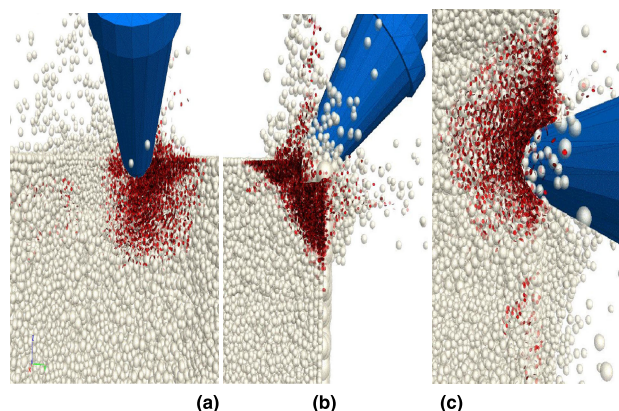


FIGURE 7. Shear fracture between coal and rock particles. (a) X-directional view of shear fracture. (b) Y-directional view of shear fracture. (c) Z-directional view of shear fracture.

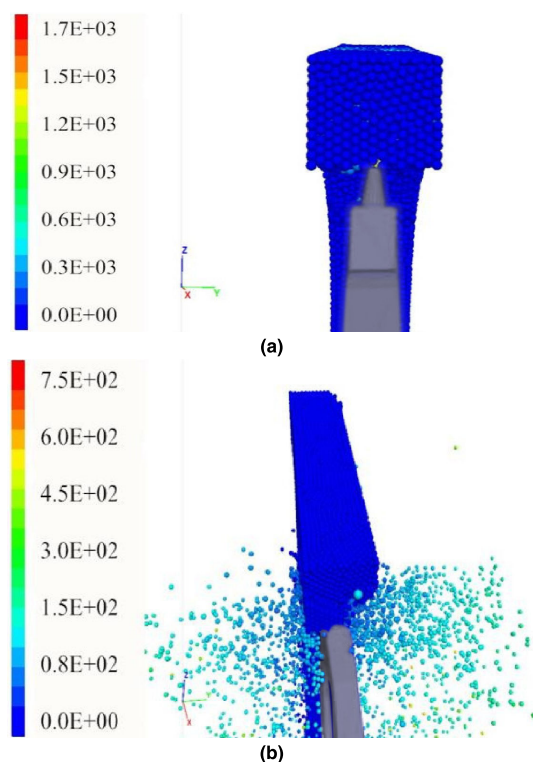


FIGURE 8. Coal and rock fragmentation. (a) Contact between the pick and coal and rock mass. (b) Coal and rock fragmentation.

different colors represent the different velocities of coal and rock particles.

From Fig. 8, it can be seen that, when the pick impacts the coal and rock mass at a certain speed, with the increase of the cut-in depth, the coal and rock mass continue to break up, and the bonding between the particles is thoroughly destroyed. Then, the coal and rock particles show the phenomenon of falling off, and the remaining coal and rock mass continue to be cut. In addition, the process is consistent with Evans' theory of fragmentation [36].

The above research proves the feasibility of using the compiled contact model to study the fragmentation of the discrete element method from both micro and macro perspectives. Therefore, the contact model between coal and rock particles is set as the developed JKR contact model. In EDEM software, 2.6×10^8 coal and rock granules are produced by adding granular factories. Among them, the radius of coal and rock granules obeys a normal distribution with a standard deviation of 0.171 and mean of 28 mm. All coal and rock granules form coal walls in the form of stacking and extrusion. The entire construction of the coal wall is completed in 10 s after the beginning of the simulation [37]–[39]. The three-dimensional model of the shearer established by UG is imported into the discrete element software EDME to study the discrete element method of the coal mining process (Fig. 9). In addition, according to the relevant requirements of coal mining technology, the Grid Bin Group corresponding to the size of the scraper conveyor is set under the shearer, and the coal and rock particles falling into it are divided into network statistics. The simulation after all of the settings is shown in Fig. 10.

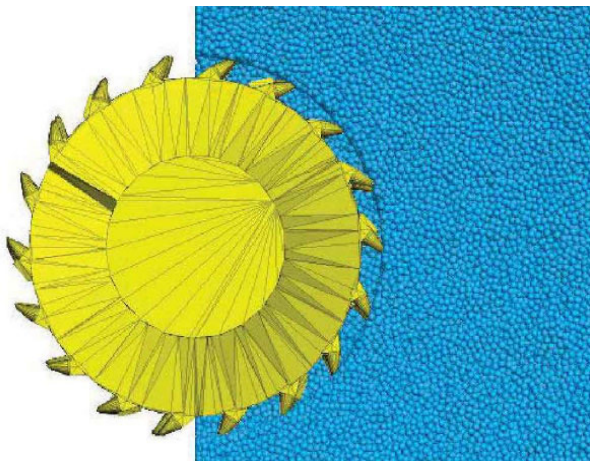


FIGURE 9. Shearer in EDEM software.

C. FACTORS AND INDICATORS OF THE SIMULATION TEST

The evaluation indexes of the working performance of the shearer in this study include the coal mining rate (C) and specific energy consumption of cutting (J). The mining rate (C) is:

$$C = \frac{n_c}{N} \tag{13}$$

In the formula, C is the coal mining rate; n_c is the number of coal and rock particles falling into the corresponding mesh of the scraper conveyor size; and N is the number of coal and rock particles in the cut coal wall [40].

The specific energy consumption of cutting (J) is:

$$J = \frac{\rho_c t n T_c}{9550 \times 3600 m_c} \tag{14}$$

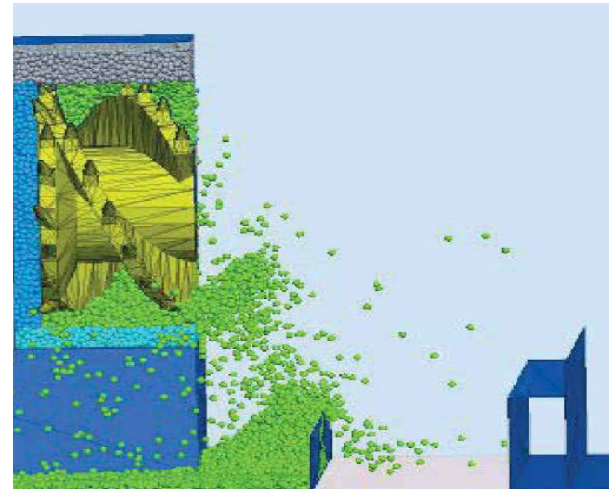


FIGURE 10. Cutting state of particle statistics at a time.

TABLE 3. Factor horizontal coding.

Code	Factor		
	Drum speed $X_1/(r/min)$	Hub diameter $X_2/(mm)$	Pick angle $X_3/(^\circ)$
1.682	80	430	24
1	72	390	21.5
0	60	330	18
-1	48	270	14.5
-1.682	40	230	12

In the formula, ρ_c is the density of coal and rock particles, kg/m^3 ; t is the working time of the shearer, s; n is the speed of the shearer drum, r/min; T_c is the drum torque of the shearer; and m_c is the quality of the cut coal and rock, kg.

According to the above theoretical analysis and previous research, reasonable control of the range of test factors is repeated 20 times per test. The average value of each test is taken as the test result. The factor level coding is shown in Table 3, and the test scheme and results are shown in Table 4.

D. MINING RATE

A quadratic regression equation model is established by using the discrete element method simulation results of the coal mining rate in Table 4 with SPSS software.

$$C = -171.997 + 3.293X_1 + 0.916X_2 + 0.586X_3 - 0.003X_1X_2 + 0.005X_1X_3 - 0.004X_2X_3 - 0.021X_1^2 - 0.001X_2^2 + 0.013X_3^2$$

Nonlinear regression analysis of the coal mining rate is carried out (Table 5).

Looking in the F table yields $F_{0.01}(10, 13) = 4.10$, $F = 24637.621 > F_{0.01}(10, 13)$, so the regression equation is significant.

The three-dimensional contour map of the factors studied is obtained by programming with MATLAB as shown in Fig. 11.

TABLE 4. Test scheme and results.

Serial number	Drum speed X_1	Hub diameter X_2	Pick angle X_3	Coal mining rate C/%	Specific energy consumption of cutting $J/(w \cdot h/m^3)$
1	1	1	1	70.47	673.38
2	1	1	-1	72.91	596.84
3	1	-1	1	75.78	586.66
4	1	-1	-1	73.13	701.70
5	-1	1	1	75.54	932.89
6	-1	1	-1	76.63	789.97
7	-1	-1	1	72.08	1136.44
8	-1	-1	-1	72.15	1152.01
9	1.682	0	0	70.28	692.57
10	-1.682	0	0	72.85	1076.04
11	0	1.682	0	71.36	705.39
12	0	-1.682	0	69.11	1224.30
13	0	0	1.682	80.97	613.86
14	0	0	-1.682	80.78	612.03
15	0	0	0	80.42	634.92
16	0	0	0	80.86	623.02
17	0	0	0	81.15	586.41
18	0	0	0	79.18	722.77
19	0	0	0	80.63	637.66
20	0	0	0	79.51	698.06
21	0	0	0	80.97	595.56
22	0	0	0	81.14	589.15
23	0	0	0	80.16	677.92

TABLE 5. Testing table of the regression equation of the mining rate.

Source	Sum of squares	Freedom	Mean square	F value
Regression	136339.076	10	13564.442	24637.621
Residual	7.003	13	0.551	
Before correction	136429.576	23		
After correction	420.976	22		

Fig. 11 shows that, when the drum speed is fixed at the zero level and the diameter of the drum hub increases gradually, the coal mining rate increases sharply at first and then decreases slowly. When the drum diameter is fixed at the zero level, the coal mining rate increases first and then decreases when the drum speed begins to increase gradually. When the hub diameter is fixed at the zero level, with the increase of the pick lift angle, the coal mining rate shows a slow rising phenomenon; when the pick lift angle is fixed at the zero level, with the increase of the hub diameter, the coal mining rate shows a sharp rise first and then a slow decline. When the drum speed is fixed at the zero level, with the increase of the pick lift angle, the coal mining rate shows a slow decline; when the pick lift angle is fixed at the zero level, with the increase of the drum speed, the coal mining rate shows a phenomenon of first rising and then falling. Through the quadratic regression equation model and Fig. 11, it can be seen that the order of the three factors influencing the notability of the shearer mining rate in the test range is as follows: the drum speed has the greatest influence on the mining rate, the drum hub diameter takes second place, and the pick angle has the least influence on the mining rate. The

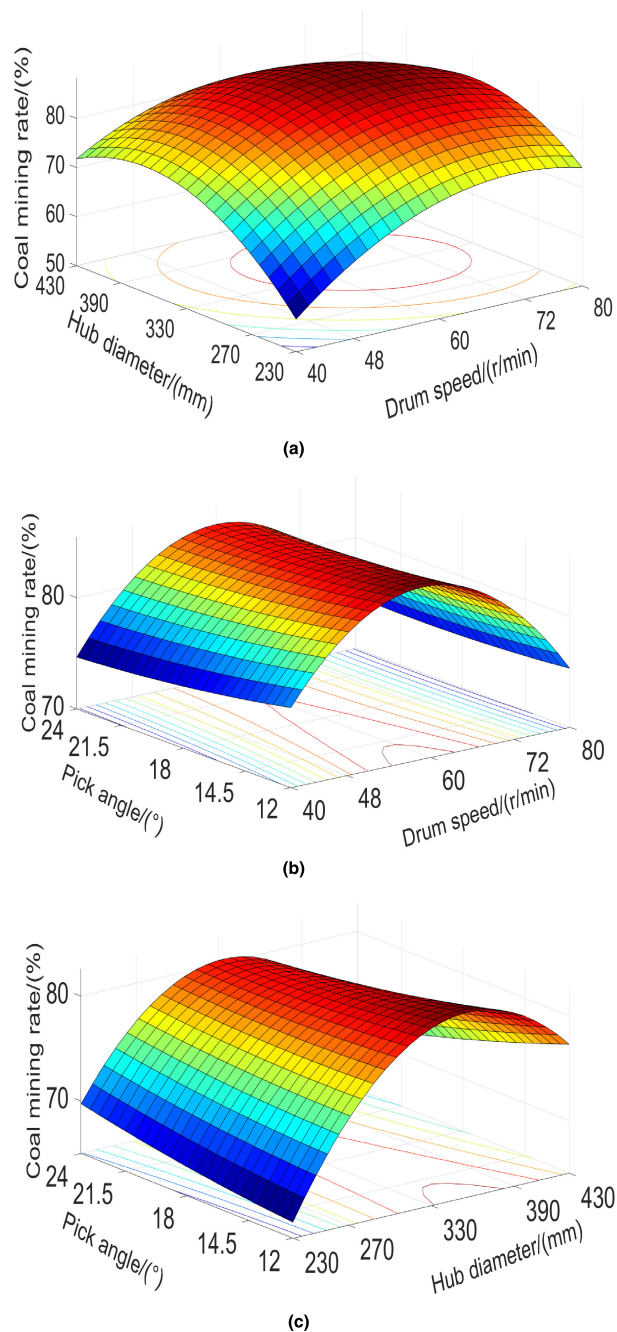


FIGURE 11. Isogram of the mining rate. (a) Pick angle at zero level. (b) Hub diameter at zero level. (c) Drum speed at zero level.

results provide a theoretical reference and basis for future research and improvement of the coal mining rate in actual production and rational selection of the shearer drum speed, drum hub diameter, and pick angle; a new method and idea for researching the shearer coal mining rate are also provided.

E. SPECIFIC ENERGY CONSUMPTION OF CUTTING

A quadratic regression equation model is established by using the discrete element method simulation results of the specific

energy consumption of cutting in Table 4 with SPSS software.

$$J = 9862.171 - 98.518X_1 - 29.326X_2 - 2.011X_3 + 0.098X_1X_2 - 0.472X_1X_3 + 0.215X_2X_3 + 0.581X_1^2 + 0.029X_2^2 - 0.996X_3^2$$

Nonlinear regression analysis of the specific energy consumption of cutting was carried out (Table 6).

TABLE 6. Checklist of regression equations for the cutting specific energy consumption.

Source	Sum of squares	Freedom	Mean square	F value
Regression	1.341×10^7	10	1.315×10^6	293.971
Residual	5.703×10^4	13	4473.231	
Before correction	1.331×10^7	23		
After correction	8.903×10^5	22		

Looking in the F table yields $F_{0.01}(10, 13) = 4.10$, $F = 293.971 > F_{0.01}(10, 13)$, so the regression equation is significant.

MATLAB was used to draw the three-dimensional contour map shown in Fig. 12.

Analysis of Fig. 12 shows that, when the drum speed is fixed at the zero level and the diameter of the drum hub increases gradually, the specific energy consumption of cutting decreases sharply at first and then slowly increases to a flat level; when the diameter of the hub is fixed at the zero level, the rotational speed of the drum increases gradually, and the cutting specific energy consumption first decreases and then increases. When the hub diameter is fixed at the zero level, the cutting specific energy consumption increases slightly at first and then decreases slightly when the lift angle of the pick begins to increase gradually. When the lift angle of the pick is fixed at the zero level, the hub diameter increases gradually, and the cutting specific energy consumption decreases sharply at first and then increases slowly. When the rotary speed of the drum is fixed at the zero level, the specific energy consumption of cutting increases slightly at first and then decreases slightly when the lifting angle of the pick begins to increase gradually. When the lifting angle of the pick is fixed at the zero level, the rotary speed of the drum increases gradually, and the specific energy consumption of cutting decreases sharply at first and then increases slowly. Through the quadratic regression equation model and Fig. 12, it can be seen that the order of the three factors influencing the notable energy consumption of shearer cutting ratio in the test range is as follows: the drum speed has the greatest influence on the energy consumption of cutting ratio, the hub diameter takes second place, and the pick angle has the least influence on the energy consumption of cutting ratio. The results provide theoretical reference and basis for future research and reduction of the specific energy consumption in actual production and rational selection of the shearer drum speed, hub diameter, and pick angle; a new method and idea for researching the specific energy consumption of the shearer are also provided.

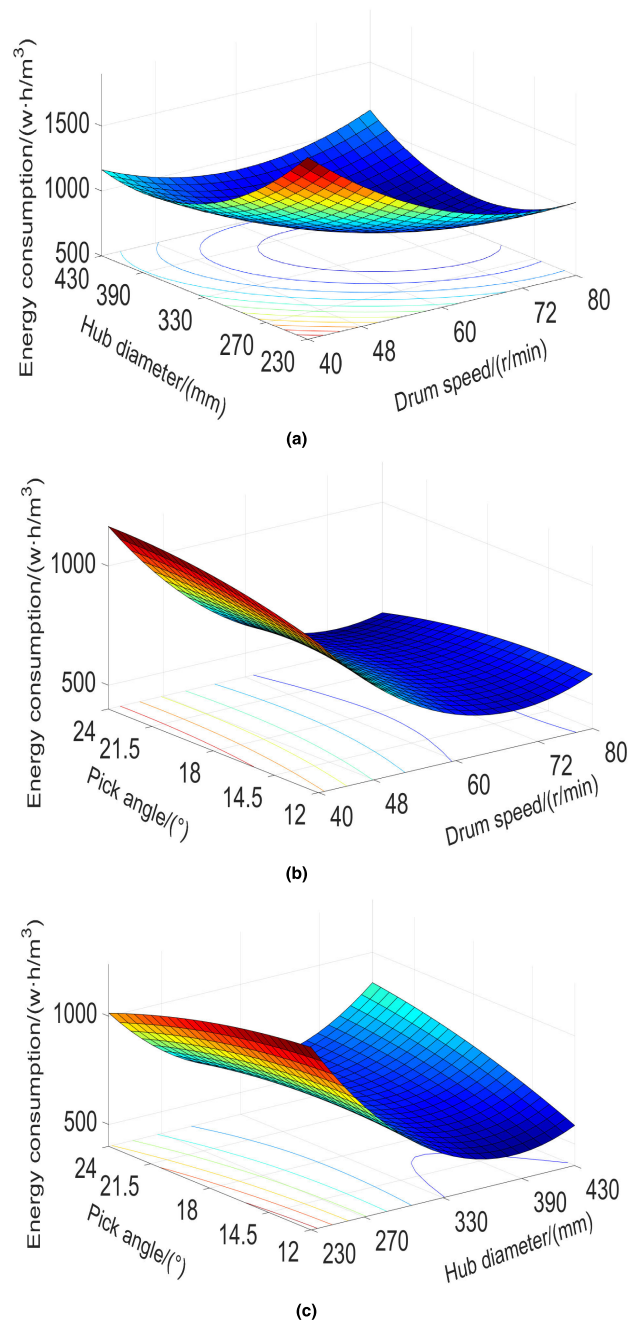


FIGURE 12. Isogram of the specific energy consumption for truncation. (a) Pick angle at zero level. (b) Hub diameter at zero level. (c) Drum speed at zero level.

F. PERFORMANCE OPTIMIZATION OF THE SHEARER

A constraint function is suggested through the regression equation of the design criterion of the fully mechanized mining area and the evaluation index of the shearer performance:

$$F_{(max)} = C - J$$

$$s.t. \begin{cases} 40r/min \leq X_1 \leq 80r/min \\ 230mm \leq X_2 \leq 430mm \\ 12^\circ \leq X_3 \leq 24^\circ \end{cases} \quad (15)$$

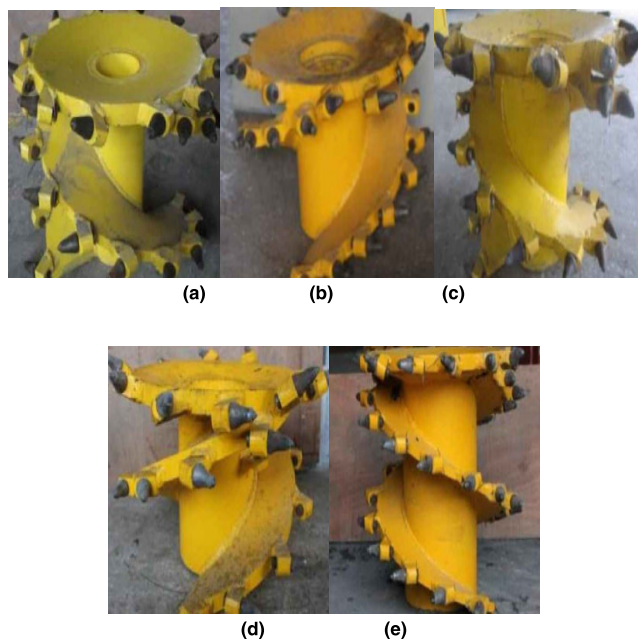


FIGURE 13. Different hub diameters. (a) Hub diameter is 230 mm. (b) Hub diameter is 270 mm. (c) Hub diameter is 330 mm. (d) Hub diameter is 390 mm. (e) Hub diameter is 430 mm.

The optimization process is carried out by the nonlinear optimization function `fmincon` and a program in MATLAB. Finally, the drum speed after rounding is 74.1 r/min, the hub diameter after rounding is 321.8 mm, and the pick lift angle after rounding is 22.3°. Under these conditions, the simulation validation test is carried out, and the results show that the coal mining rate is 80.71% and that the cutting specific energy consumption is 585.64 w · h/m³.

IV. TEST VERIFICATION

When the lift angle of the pick is 18° and the diameter of the hub is 230 mm, 270 mm, 330 mm, 390 mm and 430 mm (Fig. 13), the shearer’s motor speed is 40 r/min, 48 r/min, 60 r/min, 72 r/min and 80 r/min, respectively, by means of the frequency converter so that the shearer can carry out the mining test on the artificial coal wall (it was previously introduced that the artificial coal wall is made by mixing coal powder, rock, and water in a 5:2:1 ratio) (Fig. 14). The results of the experiment and simulation are shown in Fig. 15 and Fig. 16.

From Fig. 15 and Fig. 16, it can be seen that, with the increase of the rotational speed, the change trends of the test and simulation coal mining rate and cutting specific energy consumption are basically the same under different hub diameters. When the rotational speed is different or the diameter of the hub is different, the coal mining rate obtained by the test is slightly smaller than that obtained by the simulation. The main reason for this phenomenon is that, because there are many crevices in each mechanism of the test bed, it is impossible to clean up completely and measure the quality of all the coal and rock falling into the scraper conveyor.



FIGURE 14. Shearer mining artificial coal wall.

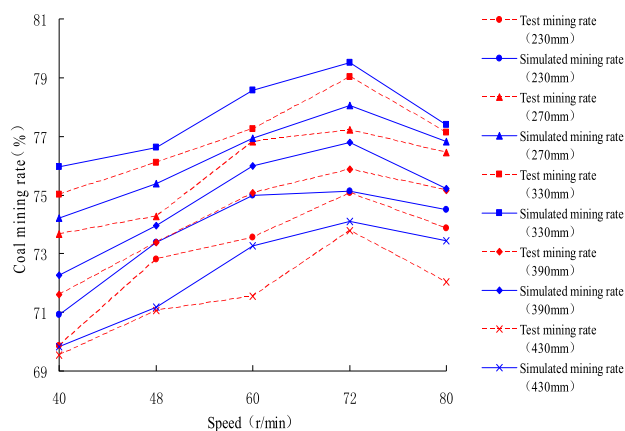


FIGURE 15. Bench test and discrete element method simulation of the coal mining rate.

Therefore, the coal mining rate obtained by the test mining is slightly smaller than that obtained by the simulation. With the same hub diameter, when the speed is lower than 72 r/min, the simulation and experimental coal recovery rates increase with the increase of shearer speed. When the rotational speed is higher than 72 r/min, with the increase of the shearer rotational speed, the simulation and experimental mining rates gradually decrease, and the maximum difference between the test and simulation mining rates is 1.71%. When the rotational speed is different or the diameter of the hub is different, the cutting specific energy consumption obtained by the test is slightly larger than that obtained by the simulation. The main reason for this phenomenon is that there are errors in the processing of the diameter of the hub in the test; it cannot reach the set value completely, and there is friction between the transmission components of each mechanism in the transmission process. Cutting coal and rock of the same volume is formed, and the specific energy consumption of the test cutting is slightly larger than that of the simulation cutting. Under the same hub diameter, when the speed is lower than 72 r/min, the specific energy consumptions of

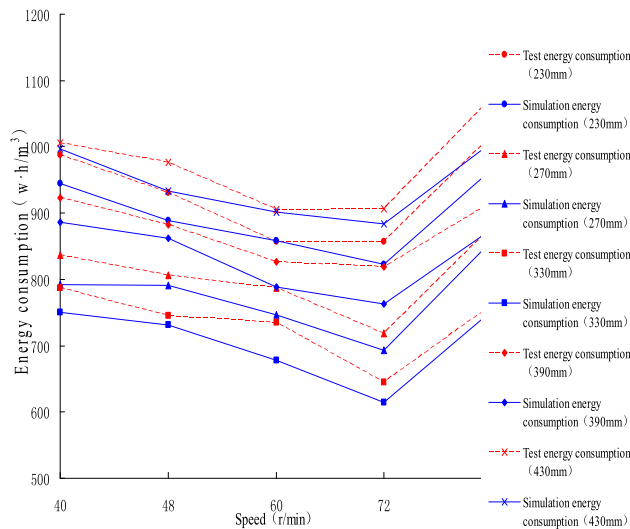


FIGURE 16. Bench test and discrete element method simulation of the specific energy consumption of cutting.

the simulation and test cutting decrease with the increase of shearer speed. When the speed of the shearer is higher than 72 r/min, the shearer speed increases continuously, and the specific energy consumptions of the simulation and test cuts increase gradually. The maximum difference between the test and simulation results is $55.65 \text{ w}\cdot\text{h}/\text{m}^3$. The two results are basically in agreement, which proves the feasibility of studying the shearer's coal mining rate and energy consumption by the discrete element method.

V. CONCLUSION

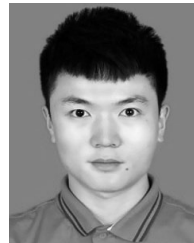
To improve the shearer's mining rate and reduce the specific energy consumption of cutting, the optimal combination of motion parameters and geometric parameters of the shearer is studied by using the discrete element method. Through the analysis of the movement model of coal particles on the pick and blade, the main factors affecting the coal mining rate and cutting specific energy consumption are determined: the rotational speed of the drum, the diameter of the hub, and the lift angle of the pick. The feasibility of using the compiled JKR contact model for coal and rock fragmentation is analyzed by EDEM discrete element software. EDEM numerical simulation provides a new idea and method for the study of shearer mining efficiency and energy consumption, which has important theoretical significance and strong engineering application value. In addition, the regression equation of the coal mining rate and cutting specific energy consumption is established, and the corresponding response surface is obtained. It is concluded that the drum speed has the greatest influence on the coal mining rate, that the drum hub diameter takes second place and that the pick lift angle has the least effect on the coal mining rate; the drum speed has the greatest influence on the cutting specific energy consumption, the drum hub diameter takes second place, and the pick lift angle has the least effect on the cutting specific energy

consumption. By optimizing the energy consumption of the coal mining rate and cutting ratio, the optimal combination of parameters after shearer rounding is obtained: the rotational speed of the drum is 74.1 r/min, the diameter of the drum hub is 321.8 mm, the angle of the pick lift is 22.3° , the coal mining rate is 80.71%, and the specific energy consumption of cutting is $585.64 \text{ w}\cdot\text{h}/\text{m}^3$. According to the comparison of the bench test and EDEM virtual simulation test results, there are some deviations in numerical value between the simulation and test results, but the change trends and the relationship between them are consistent. Therefore, it is feasible to use the discrete element method to analyze and optimize the energy consumption of the shearer's mining rate and cutting ratio, and the research results provide a theoretical reference and basis for the rational design and selection of the shearer's motion parameters and geometric parameters in the future.

REFERENCES

- [1] S. Hao, S. Wang, R. Malekian, B. Zhang, W. Liu, and Z. Li, "A geometry surveying model and instrument of a scraper conveyor in unmanned longwall mining faces," *IEEE Access*, vol. 5, pp. 4095–4103, 2017.
- [2] J. Brodny, S. Alszar, J. Krystek, and M. Tutak, "Availability analysis of selected mining machinery," *Arch. Control Sci.*, vol. 27, no. 2, pp. 197–209, Jun. 2017.
- [3] D. Szurgacz and J. Brodny, "Innovative visualization system designed to monitor parameters of mining systems operation," *Multidisciplinary Aspects Prod. Eng.*, vol. 1, no. 1, pp. 361–368, Oct. 2018.
- [4] J. Mukherjee, J. Mukherjee, D. Chakravarty, and S. Aikat, "A novel index to detect opencast coal mine areas from landsat 8 OLI/TIRS," *IEEE J. Sel. Topics Appl. Earth Observ. Remote Sens.*, vol. 12, no. 3, pp. 891–897, Mar. 2019.
- [5] H. Yang, W. Li, C. Luo, J. Zhang, and Z. Si, "Research on error compensation property of strapdown inertial navigation system using dynamic model of shearer," *IEEE Access*, vol. 4, pp. 2045–2055, 2016.
- [6] J. Brodny, M. Tutak, and A. John, "Analysis of influence of types of rocks forming the goaf with caving on the physical parameters of air stream flowing through these gob and adjacent headings," *Mech. Fluids Gases*, vol. 24, no. 1, pp. 43–49, Jan. 2018.
- [7] V. B. Prush and R. B. Lohman, "Time-varying elevation change at the centralia coal mine in centralia, Washington (USA), constrained with InSAR, ASTER, and optical imagery," *IEEE J. Sel. Topics Appl. Earth Observ. Remote Sens.*, vol. 8, no. 2, pp. 919–925, Feb. 2015.
- [8] C. Carasco, B. Pérot, J.-L. Ma, H. Toubon, A. Dubille-Auchère, and A. Lyoussi, "Improving gross count gamma-ray logging in uranium mining with the NGRS probe," *IEEE Trans. Nucl. Sci.*, vol. 65, no. 3, pp. 919–923, Mar. 2018.
- [9] J. Currie, R. R. Bond, P. McCullagh, P. Black, D. D. Finlay, and A. Peace, "Eye tracking the visual attention of nurses interpreting simulated vital signs scenarios: Mining metrics to discriminate between performance level," *IEEE Trans. Human-Mach. Syst.*, vol. 48, no. 2, pp. 113–124, Apr. 2018.
- [10] X. Fan, R. Y. Da Xu, L. Cao, and Y. Song, "Learning nonparametric relational models by conjugately incorporating node information in a network," *IEEE Trans. Cybern.*, vol. 47, no. 3, pp. 589–599, Mar. 2017.
- [11] L. Cheng, B. Van Dongen, and W. Van Der Aalst, "Scalable discovery of hybrid process models in a cloud computing environment," *IEEE Trans. Services Comput.*, to be published.
- [12] Y. Wang, H. Li, L. Cheng, and X. Li, "A QoS-QoR aware CNN accelerator design approach," *IEEE Trans. Comput.-Aided Design Integr. Circuits Syst.*, to be published.
- [13] A. M. Dizqah, B. Lenzo, A. Sornioti, P. Gruber, S. Fallah, and J. De Smet, "A fast and parametric torque distribution strategy for four-wheel-drive energy-efficient electric vehicles," *IEEE Trans. Ind. Electron.*, vol. 63, no. 7, pp. 4367–4376, Jul. 2016.

- [14] S. B. Eryilmaz, E. Neftci, S. Joshi, S. Kim, M. BrightSky, H.-L. Lung, C. Lam, G. Cauwenberghs, and H.-S. P. Wong, "Training a probabilistic graphical model with resistive switching electronic synapses," *IEEE Trans. Electron Devices*, vol. 63, no. 12, pp. 5004–5011, Dec. 2016.
- [15] L. Sheng, W. Li, Y. Wang, M. Fan, and X. Yang, "Sensorless control of a shearer short-range cutting interior permanent magnet synchronous motor based on a new sliding mode observer," *IEEE Access*, vol. 5, pp. 18439–18450, 2017.
- [16] O. J. Abdel-Baqi, A. Nasiri, and P. J. Miller, "Energy management for an 8000 HP hybrid hydraulic mining shovel," *IEEE Trans. Ind. Appl.*, vol. 52, no. 6, pp. 5041–5050, Nov./Dec. 2016.
- [17] K. Cai, H. Xie, and J. S. C. Lui, "Information spreading forensics via sequential dependent snapshots," *IEEE/ACM Trans. Netw.*, vol. 26, no. 1, pp. 478–491, Feb. 2018.
- [18] K. A. Miller, J. D. Luck, D. M. Heeren, T. Lo, D. L. Martin, and J. B. Barker, "A geospatial variable rate irrigation control scenario evaluation methodology based on mining root zone available water capacity," *Precis. Agricult.*, vol. 19, no. 4, pp. 666–683, Aug. 2018.
- [19] Y. Li, T.-H. Yang, H.-L. Liu, X.-G. Hou, and H. Wang, "Effect of mining rate on the working face with high-intensity mining based on microseismic monitoring: A case study," *J. Geophys. Eng.*, vol. 14, no. 2, pp. 350–358, Feb. 2017.
- [20] J. Freebairn, "Mining booms and the exchange rate," *Austral. J. Agricult. Resource Econ.*, vol. 59, no. 4, pp. 533–548, Oct. 2015.
- [21] O. Sdvyzhkova and R. Patyńska, "Effect of increasing mining rate on longwall coal mining—Western donbass case study," *Studia Geotechnica et Mechanica*, vol. 38, no. 1, pp. 91–98, Mar. 2016.
- [22] K. Svobodova, P. Sklenicka, and J. Vojar, "How does the representation rate of features in a landscape affect visual preferences? A case study from a post-mining landscape," *Int. J. Mining, Reclamation Environ.*, vol. 29, no. 4, pp. 266–276, Jul. 2015.
- [23] F. Arteaga, M. Nehring, and P. Knights, "The equipment utilisation versus mining rate trade-off in open pit mining," *Int. J. Mining, Reclamation Environ.*, vol. 32, no. 7, pp. 495–518, Oct. 2018.
- [24] M. A. Tyulenev, T. N. Gvozdkova, S. A. Zhironkin, and E. A. Garina, "Justification of open pit mining technology for flat coal strata processing in relation to the stratigraphic positioning rate," *Geotech. Geol. Eng.*, vol. 35, no. 1, pp. 203–212, Feb. 2017.
- [25] Y. W. Chang, J. Luo, J. Chen, L. Xu, Z. Chai, S. Wang, Y. Dong, and X. Wang, "Compact model for tunnel diode body contact SOI n-MOSFETs," *IEEE Trans. Electron Devices*, vol. 66, no. 1, pp. 249–254, Jan. 2019.
- [26] V. S. Shagapov, O. A. Shepelkevich, and A. V. Yalaev, "The initial stage of hydrate formation in liquid volume on impurity particles upon contact of gas and water," *Theor. Found. Chem. Eng.*, vol. 51, no. 4, pp. 448–457, Jul. 2017.
- [27] M. Molina, P. Castelli, and G. Foddiss, "Web traffic modeling exploiting TCP connections' temporal clustering through HTML-REDUCE," *IEEE Netw.*, vol. 14, no. 3, pp. 46–55, May/June. 2000.
- [28] K. Mitsufuji, M. Nambu, K. Hirata, and F. Miyasaka, "Numerical method for the ferromagnetic granules utilizing discrete element method and method of moments," *IEEE Trans. Magn.*, vol. 54, no. 3, Mar. 2018, Art. no. 7000504.
- [29] N. Mahdinejad, H. O. Mota, E. J. Silva, and R. Adriano, "Improvement of system quality in a generalized finite-element method using the discrete curvelet transform," *IEEE Trans. Magn.*, vol. 53, no. 6, Jun. 2017, Art. no. 7203704.
- [30] K. D. Gao, "Study on coal-loading performance of thin coal seam shearer," Ph.D. dissertation, School Mechatronic Eng., China Univ. Mining Technol., Xuzhou, China, 2014.
- [31] J. Li, B. Whisner, and J. A. Waynert, "Measurements of medium-frequency propagation characteristics of a transmission line in an underground coal mine," *IEEE Trans. Ind. Appl.*, vol. 49, no. 5, pp. 1984–1991, Sep./Oct. 2013.
- [32] E. Ahmed, I. Yaqoob, A. Gani, M. Imran, and M. Guizani, "Internet-of-Things-based smart environments: State of the art, taxonomy, and open research challenges," *IEEE Wireless Commun.*, vol. 23, no. 5, pp. 10–16, Oct. 2016.
- [33] L. Zhang, X. Xia, and J. Zhang, "Medium density control for coal washing dense medium cyclone circuits," *IEEE Trans. Control Syst. Technol.*, vol. 23, no. 3, pp. 1117–1122, May 2015.
- [34] W. Saad, Z. Han, H. V. Poor, and T. Basar, "Game-theoretic methods for the smart grid: An overview of microgrid systems, demand-side management, and smart grid communications," *IEEE Signal Process. Mag.*, vol. 29, no. 5, pp. 86–105, Sep. 2012.
- [35] J. Chirinos, D. Oropeza, J. González, V. Zorba, and R. E. Russo, "Analysis of plant leaves using laser ablation inductively coupled plasma optical emission spectrometry: Use of carbon to compensate for matrix effects," *Appl. Spectrosc.*, vol. 71, no. 4, pp. 709–720, Apr. 2017.
- [36] I. Evans, "A theory of the cutting force for point-attack picks," *Int. J. Mining Eng.*, vol. 2, no. 1, pp. 63–71, Mar. 1984.
- [37] G. Liu, W. Sun, S. M. Lowinger, Z. Zhang, M. Huang, and J. Peng, "Coupled flow network and discrete element modeling of injection-induced crack propagation and coalescence in brittle rock," *Acta Geotechnica*, vol. 14, no. 3, pp. 843–868, Jun. 2019.
- [38] M.-L. Maier, T. Henn, G. Thaeter, H. Nirsch, and M. J. Krause, "Multi-scale simulation with a two-way coupled lattice Boltzmann method and discrete element method," *IEEE Trans. Electron Devices*, vol. 40, no. 9, pp. 1591–1598, Jun. 2017.
- [39] S. M. Binesh, E. Eslami-Feizabad, and R. Rahmani, "Discrete element modeling of drained triaxial test: Flexible and rigid lateral boundaries," *Int. J. Civil Eng.*, vol. 16, no. 10, pp. 1463–1474, Oct. 2018.
- [40] C.-W. Lin, J.-S. Wang, and P.-C. Chung, "Mining physiological conditions from heart rate variability analysis," *IEEE Comput. Intell. Mag.*, vol. 5, no. 1, pp. 50–58, Feb. 2010.



ZHIZHONG XING received the B.S. degree from the Inner Mongolia University of Science and Technology and the M.S. degree from Yunnan Agricultural University, in 2014 and 2017, respectively. He is currently pursuing the Ph.D. degree with the College of Mechanical Engineering, Xi'an University of Science and Technology, China. His research interests include digital product design of coal mine machinery and the discrete element method.



WEI GUO is currently a Professor, a Ph.D. Supervisor, and a Ph.D. Leader in mechanical manufacturing and automation with the Xi'an University of Science and Technology, Xi'an, China. He is a famous Teacher of teaching in Shaanxi province and Shaanxi province sanqin talents. He is a Station Master of postdoctoral research mobile station of mechanical engineering. He has received two Provincial Science and Technology Awards, one Municipal Science and Technology Award, and two Provincial Teaching Achievement Awards. His research interests include coal mine machinery and its automation and digitized products of coal mine machinery.

• • •